University of Tartu

Faculty of Science and Technology

Institute of Technology

Kristin Kandelin

Development of the Battery Management Subsystem for the SUTS picosatellite

Bachelor's thesis (12 ECTS)

Computer Engineering

Supervisors:

Mari Allik MSc

Kristo Allaje MSc

Tartu 2025

Abstract/Resümee

Development of the Battery Management Subsystem for the SUTS picosatellite

Satellites require reliable power sources to remain operational in space. Most satellites use a combination of primary and secondary power sources: the primary typically being solar cells, and the secondary being rechargeable batteries that supply power when the satellite is in shade. Careful design and testing of power subsystems are essential to ensure the satellite's reliable operation.

This thesis focuses on the development of the Battery Management Subsystem (BatMan) for the three-unit PocketQube Strategic Upgrades Test Satellite (SUTS). The main objectives were to define the requirements of the subsystem, identify a suitable battery candidate based on those requirements, and design and test the first prototype of BatMan. As part of the process, eight subsystem requirements were established, based on which a suitable battery was selected. The battery was tested under vacuum and short circuit to assess its suitability for use in SUTS. In addition, the first prototype of BatMan was designed, but not all functionality tests could be performed, as part of the prototype would have to be redesigned.

CERCS: T320, Space technology

Keywords: PocketQube, SUTS, ESTCube-2

Pikosatelliit SUTSu akuhalduse alamsüsteemi arendamine

Satelliitidel on kosmoses töötamiseks vaja energiat. Enamasti on satelliitide peamine energiaallikas päikesepaneelid ning tagavaraenergiaallikas akud, mida kasutatakse siis, kui satelliit on Päikese eest varjus. Selleks, et tagada satelliidi töökindlus, tuleb satelliidi toitealamsüsteemi disainimisele ja testimisele suurt rõhku panna.

See bakalaureusetöö keskendub 3-ühikulise PocketQube'i SUTSu (Strateegiliste Uuenduste Testimise Satelliit) toitealamsüsteemi disainile. Töö peamisteks eesmärkideks oli töötada välja akuhalduse alamsüsteemi (BatMan) nõuded, leida nende nõuete järgi sobivad akukandidaadid ning seejärel disainida nende akukandidaatidega BatMani esimene prototüüp. Töö käigus töötati BatMani jaoks välja kaheksa nõuet ning leiti nende järgi sobiv akukandidaat. Akukandidaadiga tehti vaakum- ja lühiseteste, et saada aru, kas see on SUTSu jaoks sobilik. Lisaks disainiti esimene BatMani prototüüp, kuid kõikide funktsionaalsustestide tegemiseni ei jõutud, kuna osa prototüübist on vaja ümber disainida.

CERCS: T320, Kosmosetehnoloogia

Võtmesõnad: PocketQube, SUTS, ESTCube-2

Contents

Abstract/Resümee **2**

List of Figures **6**

List of Tables **7**

Acronyms **8**

1 Introduction **9**

2 Battery theory **11**

2.1 Batteries as secondary power sources in spacecraft 11

2.2 Lithium batteries 11

2.3 Testing batteries for space applications 13

3 Subsystem overview **15**

3.1 Battery Management Subsystem (BatMan) 15

3.2 Requirement specification 15

4 Battery cell selection and testing **18**

4.1 Battery candidate selection 18

4.2 Battery cell testing 19

4.2.1 Initial testing of the batteries in vacuum 19

4.2.2 Battery testing in a chassis 20

4.2.3 Cell short circuit testing 23

4.3 Battery cell choice 25

5 Prototype development and testing **27**

5.1 Subsystem design 27

5.1.1 Analog-to-digital converter 27

5.1.2 Battery controller 28

5.1.3 Voltage monitor 29

5.1.4 Battery cut-off switch 31

5.2 PCB design 33
5.3 PCB assembly results 33
5.3.1 Unexpected results 33
5.3.1.1 Battery controller 33
5.3.1.2 Battery cut-off switch 35

6 Conclusions and future work **38**

Acknowledgements **43**

A Battery candidates **44**

B PCB design **46**

Licence **50**

List of Figures

2.1 A lithium-ion battery's voltage, current and capacity changing over time when charging. [12] 12

3.1 High-level overview of SUTS' BatMan prototype. 15

4.1 LiPo chassis testing setup. 20
4.2 LiPo chassis testing setup in the Bacoeng vacuum bucket. 21
4.3 Li-ion cell after short test. 24
4.4 LiPo cell after short test. 25

5.1 BatMan prototype system configuration. 27
5.2 ADC circuitry configuration. 28
5.3 Battery controller circuitry configuration. 29
5.4 Battery controller voltage monitor circuitry configuration. 30
5.5 Voltage monitor switching logic. 30
5.6 Battery cut-off circuitry configuration. 32
5.7 Battery controller breakout board. 34
5.8 Battery cut-off switch breakout board. 36

B.1 Batman PCB front layer. This layer has all the components used on this PCB. . 46
B.2 Batman PCB back layer. 47
B.3 Batman PCB from the front. 48
B.4 Batman PCB from the back. 49

List of Tables

3.1 Requirements for BatMan 16

4.1 Battery characteristics before the first test 21
4.2 Battery characteristics after the first test 22
4.3 Battery characteristics before the second test 22
4.4 Battery characteristics after the second test 22
4.5 Battery characteristics before the test 24
4.6 Battery characteristics after the test 25

A.1 First 5 battery candidates 44
A.2 Last 5 battery candidates 45

Acronyms

ADC Analog-to-digital converter. ADC converts analog signals into digital signals. 27–29, 33, 38

BatMan Battery Management Subsystem. An Electrical Power System subsystem that supplies the spacecraft with power from a secondary source i.e. the batteries. 2, 7, 9, 15, 16, 18, 25, 38

DoD Depth of discharge. The percentage of the battery that has been discharged relative to the overall capacity of the cell. 14

EOCV End of charge voltage. The voltage at which a battery cell's charging process is terminated. 13

FPB Floating Power Bus. The power bus that connects the satellite's solar panels to the rest of the satellites Electrical Power System. Bus voltage in range 3 V to 4.2 V. 15, 33, 34

LEO Low Earth Orbit. LEO is defined as a distance of 100 to 2000 km from the Earth's surface. 9, 11, 14

MOSFET Metal-oxide-semiconductor field-effect transistor. It is a field-effect transistor with a MOS structure. Typically, the MOSFET is a three-terminal device with gate (G), drain (D) and source (S) terminals. 29, 31, 33–37

PCB Printed Circuit Board. A laminated sandwich structure of conductive and insulating layers, each with a pattern of traces, planes and other features etched from one or more sheet layers of copper laminated onto or between sheet layers of a non-conductive substrate. 24–26, 33–35

PCM Protection Circuit Module. A protection circuit that guards a Lithium Polymer battery against various potential risks during the battery's operation. 24, 25, 44

SUTS Strategic Upgrades Test Satellite. SUTS is a 3-unit PocketQube developed by the Estonian Student Satellite. 2, 9, 11, 15, 16, 27, 36, 38

1 Introduction

The development of standardised satellite platforms such as CubeSat [1] and PocketQube [2] has significantly expanded access to space exploration for entities beyond government-funded agencies, including university student groups. The CubeSat standard was developed in 1999 by California Polytechnic State University and Stanford University to help students learn to build, develop, and test small satellites designed to go to low Earth orbit (LEO) [3]. CubeSats are a type of nanosatellite consisting of one or multiple units of 10x10x10 cm, where one unit can have a mass of up to 2 kg [1]. The PocketQube standard, proposed in 2009 by Robert J. Twiggs, is a type of picosatellite where a unit is 5x5x5 cm and each unit can weigh up to 0.25 kg [2].

Most satellites have two power sources to keep their systems operational: primary and secondary. Solar panels are considered the primary power source for almost any type of spacecraft, producing power when the satellite is in sunlight [4]. However, once the satellite goes into shade, the solar panels stop producing power. Therefore, a secondary power source such as rechargeable batteries is used to keep the system running until the spacecraft exits the eclipse and the solar panels take over again [4].

The Strategic Upgrades Test Satellite (SUTS) is a 3-unit PocketQube nanosatellite developed by the Estonian Student Satellite Foundation, scheduled to launch to LEO in 2028. Due to its compact size and power constraints, SUTS requires a custom-designed Battery Management Subsystem (BatMan) to reliably handle power storage, protection, and monitoring. Designing a safe and efficient battery management subsystem for space is essential in order to develop a functional satellite. It must meet strict requirements for thermal behaviour, safety, stored energy capacity, and reliability, all while fitting within the tight volume and mass limits of the PocketQube format.

This thesis focuses on the design and initial validation of the BatMan prototype for SUTS. The main objectives of this thesis are:

- to define requirements for the BatMan,
- to evaluate and test battery candidates for space conditions,
- to design and implement a prototype of the BatMan.

Chapter 2 gives an overview of lithium battery characteristics and their testing procedure for space. Chapter 3 gives an overview of the BatMan and outlines its system requirements. Chapter 4 gives an overview of the battery choice and the tests performed to validate the batteries and

the design. Chapter 5 gives an overview of the design process of the first subsystem prototype and outlines the problems discovered during its testing process.

2 Battery theory

2.1 Batteries as secondary power sources in spacecraft

Satellites use various types of batteries as their secondary power source, such as silver-zinc, nickel-cadmium (also known as alkaline), and lithium-ion. Silver-zinc batteries were used mainly in the early stages of space exploration, for satellites such as Ranger-3 and Mariner-2 [5]. Their advantages include a high power and energy density and a charge efficiency of more than 99%. However, they cost a lot compared to other batteries and have a limited number of charge cycles, up to a 100 [6]. Nickel-cadmium batteries are generally used in missions where constraints on mass and volume are less critical, with an operational lifespan of two to three years. However, Ni-Cd batteries are known to perform poorly at temperatures less than -10 °C [5]. LEO can have temperatures ranging from -65 to +150 °C [7].

Lithium-ion batteries are used in space because they are compact, lightweight and have low thermal dissipation [5]. The energy density of lithium-ion batteries is estimated to be 240 Wh/L, while silver-zinc has a density of 200 Wh/L, and nickel-cadmium 100 Wh/L [8]. In addition, they are widely used in consumer products and thus readily available. There are also a lot of integrated circuits available on the market to regulate their charge and discharge, and a lot of support material is available online to ease the prototyping process. Lithium-ion batteries were also used on board ESTCube-2, which was a CubeSat previously developed by the Estonian Student Satellite Foundation, but the batteries used in the spacecraft are too large to reuse in SUTS. When taking into account the space and weight constraints of SUTS, lithium-ion batteries are the most suitable choice for further development and a suitable battery candidate must be found.

2.2 Lithium batteries

Selecting appropriate batteries for a space mission requires careful consideration of both mission-specific requirements and battery cell characteristics. Key parameters that define a battery include its nominal voltage, capacity, and charge/discharge current rate. Mission-related factors, such as operating temperature ranges and expected charge/discharge profiles, can significantly influence a battery's capacity, voltage stability, and overall operational lifespan. [9]

The nominal voltage for most lithium cells is 3.6 to 3.7 V, with the minimum cell voltage being 3 V and the maximum 4.2 V. Exceeding the battery's maximum charge limit could result in internal shorts in the cell, leading to electrolyte breakdown and increased internal pressure. Similarly, undercharging a battery cell could lead to short-circuit conditions when the cell is charged. Cell voltage is affected by temperature changes, as with lower temperatures, an increase in the battery's internal resistance and a decrease in chemical activity can be noted. [9]

Battery capacity is the total amount of energy that can be produced due to the electrochemical reactions in the battery. Battery capacity is affected by characteristics such as high state-of-charge during storage, higher discharge rates, low temperature during charging, and using the battery outside of its specified operational temperatures [9].

Charge and discharge characteristics are often represented as multiples of a C-rate. The C-rate is defined as the amount of current that will charge or discharge the battery to the cutoff voltage in one hour [10]. Battery manufacturers usually specify a battery's charge and discharge current limits in the batteries' datasheets.

The process of charging a lithium-ion battery is illustrated in Figure 2.1. When a lithium-ion battery is initially charged, its voltage increases rapidly, while its charge capacity accumulates more gradually. The battery must be charged with a constant current, often specified in its datasheet, until its capacity catches up to the voltage level. Once the voltage level reaches 4.2 V, the battery is charged with a constant voltage. In this phase, the charging current progressively decreases as the battery approaches full capacity. Upon reaching full charge, the battery must be disconnected from the charging circuit to prevent overcharging. [11]

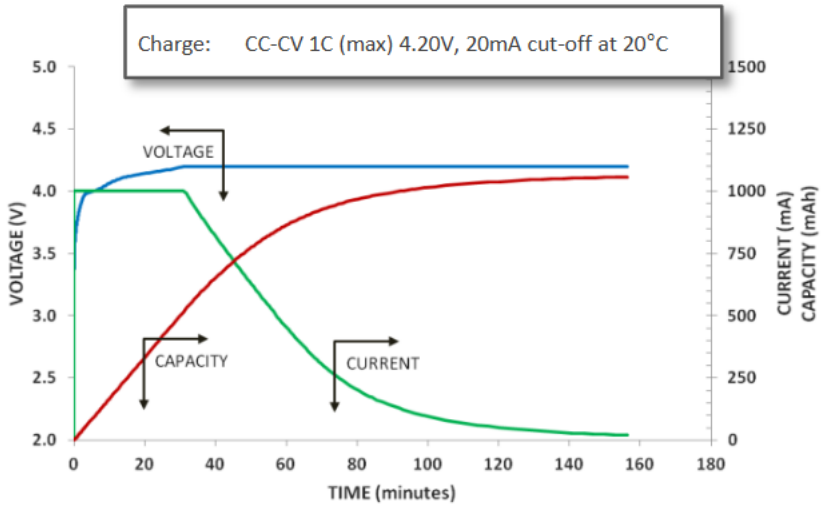

Figure 2.1. A lithium-ion battery's voltage, current and capacity changing over time when charging. [12]

2.3 Testing batteries for space applications

Battery cells must be thoroughly characterised to ensure they are fit for space and will not damage either the satellite or the carrier rocket. Satellite launch providers such as Arianespace require safety documentation about a satellite's batteries. As described by Cameron et al. [13] and the ECSS-E-HB-20-02A standard [14], it is recommended the following tests to be performed on battery cells and the circuitry surrounding them to evaluate their suitability and safety.

- External short test
- Vacuum test
- Charge and discharge cycling at room temperature
- Overcharge and discharging tests
- Battery lifetime

Short tests

External battery short tests are performed to simulate how the battery cells would behave in the event of a power bus short, where both battery terminals are shorted together. An external short-circuit test is performed by connecting the two battery terminals with a low-resistance conductive material. The test is deemed successful when the battery cell discharges fully without any battery failure. During the test, battery temperature, voltage and current should be noted down. [14]

Vacuum test

Vacuum tests are performed on battery cells to ensure that they do not leak in vacuum conditions. The batteries are measured before the test at a precision of a hundredth of a gram. The cells are then put into the test chamber for 6 hours at a constant temperature of 25°C at a constant pressure of 5 Torr (approximately 660 pascals). The batteries are weighed again after the test to check for potential electrolyte leaks. [13]

Charge and discharge cycling

Battery cycling tests are done to evaluate how charge-discharge cycles affect battery cell capacity. Before starting the test, the initial capacity of the cell must be measured. The cell should be charged at its previously specified current (usually set by manufacturers) to its end of charge voltage (EOCV). Next, the cell should be discharged at a specified current (again spec-

ified by the manufacturer) to the desired depth of discharge (DoD). Capacity checks should be performed regularly between the charge and discharge cycles. [14]

Overcharge and discharge tests

Battery overcharge and discharge tests are performed on the cell and its protective circuitry to ensure that the batteries are safe for the satellite. When battery cells are used outside of their operating range, extreme conditions can cause thermal failure, which could result in fire. [15]

The overcharge test shall be used to characterise and verify that the overcharge protection of the battery management circuitry works. The batteries shall be charged 0.3 V over their maximum charge with a current of 1.0 C until the protective circuitry stops the test or a maximum of 6 hours. The time when the protective circuitry activates shall be noted down, and current, voltage, and temperature are recorded throughout the test. [13]

Over-discharge tests would be performed in a similar manner to ensure the protective circuitry activates to preserve the battery. The battery shall be over-discharged at a constant current to 0 V. The protective circuitry should engage before that point. The time when the circuitry activates shall be noted down, and current, voltage, and temperature are recorded throughout the test. [13]

Lifetime test

Battery cycling based on the LEO profile aims to show how the battery and its surrounding circuitry would perform while it is in orbit. A generic LEO profile consists of 90-minute cycles, of which 60 minutes are spent in the Sun charging, and 30 minutes in the shade discharging (with an accurate load that would be discharging the battery). Selecting a temperature profile close to the environment in orbit is recommended. [14]

One cycle consists of 60 minutes of charging the battery according to its characteristics until it is full. The input voltage could also have a ripple to further simulate the real charging process. After the light period, there should be a 30-minute discharging time, during which it discharges at a constant current. The test should be repeated at least 10 times, and battery capacity should be measured before and after the test. [14]

3 Subsystem overview

3.1 Battery Management Subsystem (BatMan)

When SUTS is in shade and the solar panels cannot generate power, the batteries are discharged to Floating Power Bus (FPB). When the spacecraft is back in sunlight, the batteries are charged using excess power from the FPB. A high-level block diagram of BatMan is shown in Figure 3.1.

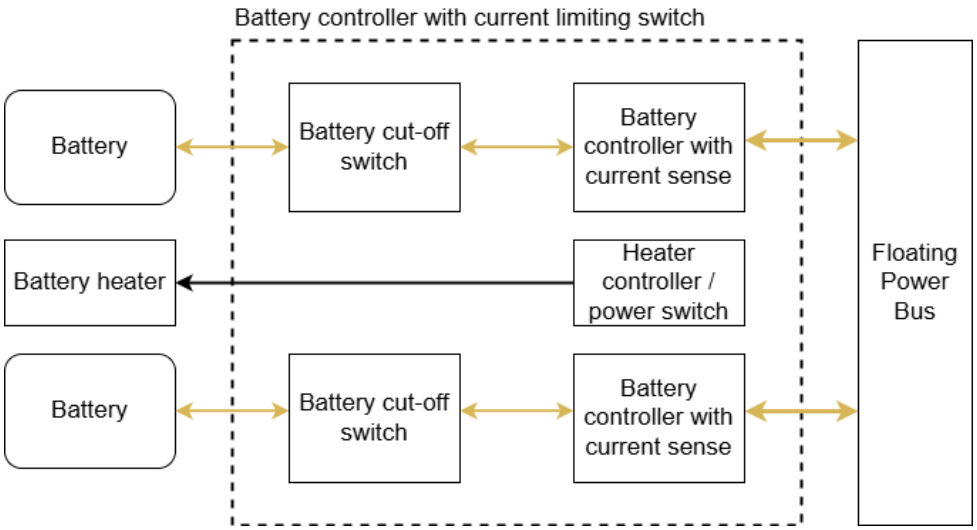

Figure 3.1. High-level overview of SUTS' BatMan prototype.

BatMan consists of three main sub-blocks: the battery cut-off switch, battery controller with a voltage monitor and current sense, and a battery heater. More information about the sub-blocks is available in Chapter 5.1. The implementation of the battery heater is outside the scope of this thesis and is not covered.

3.2 Requirement specification

The first step for development was to define requirements for the subsystem prototype. Eight requirements were created and can be seen in Table 3.1. Once the requirements had been agreed upon with the rest of the team, the search for suitable battery cell candidates could begin.

Table 3.1. Requirements for BatMan

ID	Requirement	Rationale	Verification
REQ-BATMAN-01	The batteries shall be charged and discharged via the same power line.	The SUTS spacecraft is very space-constrained and does not have room for dedicated charge and discharge paths.	Review of design
REQ-BATMAN-02	The battery management system shall be capable of electrically disconnecting batteries from the floating power bus.	To prevent the system from unwanted power ups and keep batteries from under and over charging.	Review of design, testing
REQ-BATMAN-03	The system shall have autonomous protection against overcharging and undercharging battery cells, which can be overridden by the MCU.	Offers more control over the batteries' limits, for example when depth of discharge needs to be modified in different stages of the mission.	Review of design, testing
REQ-BATMAN-04	Instantaneous currents shall be measured for both charging and discharging with 1 mA accuracy.	Some chips may operate on a mA of current. If the accuracy was 10 mA or more, the system may only notice a change in current after multiple chips have mistakenly started operating.	Review of design, testing
REQ-BATMAN-05	Battery cell voltages shall be measured with 10 mV accuracy.	Battery cells themselves are often defined with 100 mV accuracy.	Review of design, testing

REQ-BATMAN-06	The system shall measure the individual cells' temperature with 1 °C accuracy.	The satellite operates in a wide range of temperatures, meaning any temperature change less than 1 °C would not be a notable change.	Review of design, testing
REQ-BATMAN-07	The battery management system shall not discharge the batteries more than TBD% of full capacity when disconnected from the floating power bus for 6 months.	Battery health must not be affected by over-discharging while the satellite awaits its launch.	Review of design, testing
REQ-BATMAN-08	It should be possible to mechanically disconnect the batteries from the system.	Having the ability to mechanically disconnect the batteries from the rest of the system can be useful for a longer shelf life.	Review of design, testing

4 Battery cell selection and testing

4.1 Battery candidate selection

A good battery candidate has a reasonable price and is easily acquirable. Additionally, a battery cell must fit within 48x46x22 mm due to the constraints imposed on the BatMan by the structure engineers. Taking these limitations into account, suitable batteries were looked for. Battery candidates were chosen from TME, Mobix, Digikey, Farnell and Panasonic's website. After narrowing all the choices down to 10 best candidates (full list available in Appendix A), a ranking process was started to identify the most suitable choice. Batteries were evaluated in the following categories:

- capacity
- dimensions
- nominal voltage
- mass
- charge current
- discharge current
- charge temperature
- discharge temperature

The batteries were evaluated based on a weighted point system from 1 to 3, with one being the best score and three being the worst. If a certain value was unknown, it got 3 points by default. The less points a battery received, the better its ranking. The chosen battery candidates and their corresponding parameters can be seen in Appendix A. The following batteries were discarded from the trade-off:

- NCA103443 as it has no available datasheet;
- IMR18350 HIGH DRAIN as it has no available datasheet;
- USE-903439-1400 as it ships from the USA, where shipping costs around 200€, which is significantly more than the other candidates' shipping fees;
- SIEMENS 6ES7623-1AE01-5AA0 as it is very expensive (177.04€) compared to the other candidates.

Batteries ACCU-LP103740/CL, NCA673440, and the XTAR AAAs scored the best and were considered as possible battery candidates at first. However, the XTAR batteries were discarded because it

was found out that they are actually 3.7 V Li-ion batteries that have an internal DC-DC converter that converts them to 1.5 V. Additionally, NCA673440 was discarded, as the contacted battery providers did not offer that battery. A new battery, UF553443ZU by Sanyo, was found from Mobix and was chosen as a new battery candidate for its good suitability. Both ACCU-LP103740/CL and UF553443ZU were bought, and the final candidate was chosen after further testing.

4.2 Battery cell testing

4.2.1 Initial testing of the batteries in vacuum

The two chosen battery candidates were ACCU-LP103740/CL (lithium polymer) and UF553443ZU (lithium-ion). Their reaction to being in vacuum was evaluated in a Bacoeng vacuum chamber [16]. Before testing, two hypotheses were set:

- The LiPo battery will inflate while in vacuum and deflate when exposed to ambient pressure again, as it has a soft case.
- The Li-ion should remain the same because of its metal case.

First test

As one of the batteries, ACCU-LP103740/CL, is made of lithium polymer, the first test was conducted outdoors as a precaution. Both the LiPo and the Li-ion were placed in a portable vacuum chamber, and before the test, the batteries' dimensions were as follows:

- LiPo: 38.61 x 37.58 x 9.79 mm
- Li-ion: 42.26 x 33.70 x 5.21 mm

The lowest pressure was -22.5 inHg or -0.76 bar (where -1 bar is considered vacuum). During the test, the LiPo swelled considerably, but there was no noticeable change in the dimensions of the Li-ion cell. Additionally, during the test, a small increase in pressure was observed. The hypothesis was that the lid of the vacuum bucket was sealed incorrectly or that one or both of the batteries outgassed. After the test, the batteries' dimensions were as follows:

- LiPo: 38.52 x 37.63 x 9.77 mm
- Li-ion: 42.30 x 33.66 x 5.17 mm

Those changes are considered minimal and within the measurement error. Therefore, both hypotheses were confirmed.

Second test

The second test was conducted in a laboratory environment, as the LiPo was deemed safe. At first, the pressure was lowered to -0.8 bars. A slight decrease in pressure was noted with the pump and valves closed, but the reason is unknown. The pressure decreased from -0.82 bars to -0.84 bars in a span of 1 hour and 9 minutes. The pressure was further decreased to -28.5 inHg or -0.96 bar 1 hour 20 minutes into the test. Like the previous test, LiPo swelling was noted, and the Li-ion battery stayed the same. After the test, the batteries' dimensions were as follows:

- LiPo: 39.14 x 37.70 x 9.78 mm
- Li-ion: 42.41 x 33.64 x 5.18 mm

As these dimensions are within the measurement error, the hypotheses were again confirmed.

4.2.2 Battery testing in a chassis

Since it was proven that the lithium polymer batteries expand in vacuum, the next step was to find out if their expansion would be harmful to the satellite. For that, another vacuum test was performed. A chassis was assembled of three FR4 plates. Two LiPo batteries were fitted between them, mounted with double-sided tape and secured with M3 bolts. An image of the testing setup can be seen in Figure 4.1. The aim of this test was to find out if the expansion of the battery would damage the boards in any way. The test would be considered a failure if the battery swelling damaged the FR4 plates in any way, and the batteries would not be considered as possible candidates.

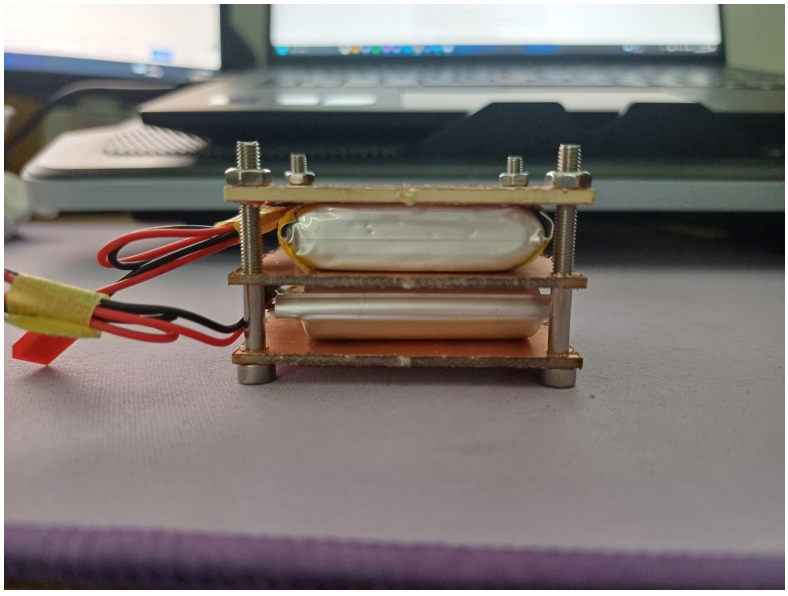

Figure 4.1. LiPo chassis testing setup.

Before starting the test, the batteries' dimensions and weight should be measured and noted down.

Additionally, the batteries' voltage should be noted down.

The chassis should be put into the vacuum chamber vertically to assess the possible swelling of the batteries better. At least two tests, both taking up 2 hours, should be conducted. The pressure should be brought down to -28.5 inHg or -0.96 bar both times. The batteries should be observed closely for the 30 minutes of the first test to assess if they fail, after that, the batteries should be checked on every 15 minutes.

After the test, battery dimensions, weight and voltage should be noted down. Additionally, the FR4 boards should be investigated to see if they got harmed during the test.

First test

Battery characteristics before the first test were as follows in Table 4.1.

Table 4.1. Battery characteristics before the first test

	ID	Dimensions (mm)	Weight (g)	Voltage (V)
Battery 1	Kapton tape	40.6x37.6x10	29.6	3.95
Battery 2	Isolation tape	42.4x37.6x9.8	29.2	3.87

The batteries were mounted in the chassis after taking their measurements and secured with double-sided tape and M3 bolts. During the test, there were no notable changes, only the batteries swelled up a bit, but that was expected. An image of the battery testing setup in the vacuum bucket can be seen in Figure 4.2.

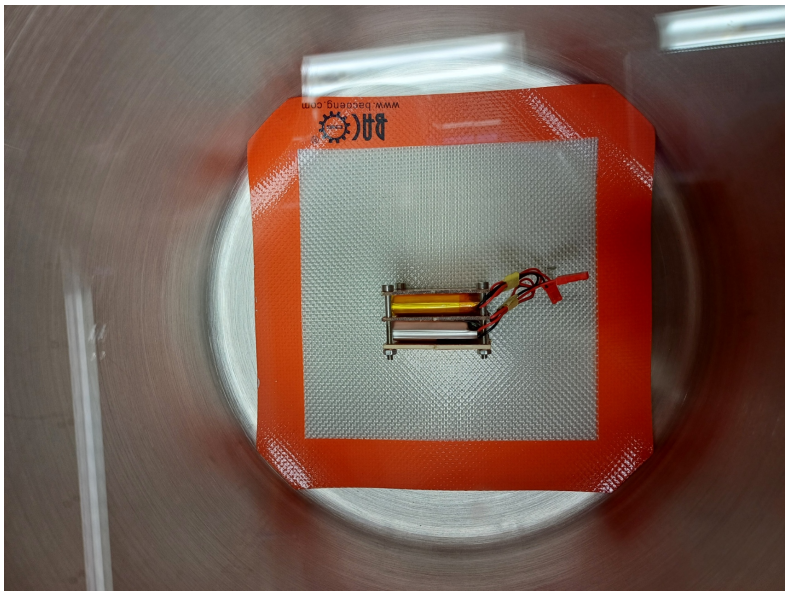

Figure 4.2. LiPo chassis testing setup in the Bacoeng vacuum bucket.

Battery characteristics after the first test were as follows in Table 4.2.

Table 4.2. Battery characteristics after the first test

	ID	Dimensions (mm)	Weight (g)	Voltage (V)
Battery 1	Kapton tape	40.2x37.7x10.3	29.7	3.95
Battery 2	Isolation tape	39.6x37.6x9.8	29.3	3.87

The removal of the double-sided tape following the test proved challenging, resulting in slight deformation of the outer casing of the batteries. However, the FR4 plates remained unaffected.

Second test

Given that the previous taping method was overly aggressive, the approach was modified for the second test by applying double-sided tape to only one side of the battery rather than both.

Battery characteristics before the second test were as follows in Table 4.3.

Table 4.3. Battery characteristics before the second test

	ID	Dimensions (mm)	Weight (g)	Voltage (V)
Battery 1	Kapton tape	40.2x37.7x10.3	29.7	3.95
Battery 2	Isolation tape	39.6x37.6x9.8	29.3	3.87

The batteries swelled up when they were in vacuum. Nothing else noteworthy happened.

Battery characteristics after the second test were as follows in Table 4.4.

Table 4.4. Battery characteristics after the second test

	ID	Dimensions (mm)	Weight (g)	Voltage (V)
Battery 1	Kapton tape	40.4x37.5x10.1	29.6	3.95
Battery 2	Isolation tape	39.1x37.9x10.0	29.4	3.87

After the batteries were removed from the vacuum chamber, the inside of the bucket smelled of battery acid. Therefore, one or both of the batteries had likely outgassed during the test. The outgassing may have been triggered either by the vacuum process itself or by the mechanical stress induced during tape removal. Additional tests could be performed to determine the exact cause. The FR4 boards remained unaffected throughout the procedure.

Conclusion

Both batteries survived the tests and remained in their original dimensions and voltages. Although batteries outgassed during the test, the cause is not certain. The batteries' expansion did not damage the FR4 chassis.

4.2.3 Cell short circuit testing

External battery short tests are performed to simulate how the battery would behave in the event of a power bus short where both battery terminals are shorted together. An external short-circuit test is done by connecting the two battery terminals with a conductive material with low resistance, such as copper wire. During the test, a fire blanket should be kept nearby in case anything goes wrong. The batteries should stay shorted until they have been safely discharged. The test is deemed successful when the battery discharges fully without any battery failure. The external battery short test is performed according to the ECSS-E-HB-20-02A [14] standard.

Before starting the test, the batteries' dimensions, weight and voltage should be measured and the batteries should be fully charged.

Pre-test procedure

A safe way for connecting the two terminals of a single battery together had to be devised. For the LiPo battery, which has both terminals on the same side, a straightforward solution would be to connect the terminals using a conductive metal element, such as a nickel strip or a large bolt. In contrast, the Li-ion battery has a different configuration, with the positive terminal located at one end and the negative terminal at the opposite end, and the battery casing serving as the positive terminal. In this case, a long nickel strip may be spot-welded to the negative terminal, then bent to make contact with the positive terminal, thereby completing the circuit.

The second step was to fully charge both batteries. For this, a benchtop power supply was be used and the batteries were charged at a constant current until the battery was almost fully charged. When the charging current started decreasing, the power supply was switched to constant voltage mode until the charging current dropped to about 5% of the cell's rated current.

Finally, the battery's dimensions, weight and voltage were measured.

Short test

Battery characteristics before the test were as follows in Table 4.5.

Table 4.5. Battery characteristics before the test

	Dimensions (mm)	Weight (g)	Voltage (V)
LiPo	39.1x37.9x10.0	29.4	4.18
Li-ion	42.41 x 33.64 x 5.18	19.2	4.16

The Li-ion test was performed by pushing the body of the battery against the nickel strip connected to the other terminal of the battery. At first, the connection caused a spark and the temperature of the connection point was rose 300 °C, followed by a rapid temperature increase in the battery itself. The test was stopped for safety at 130 °C, as it had risen by 30 °C in just a few seconds, and the battery started smoking. The terminals were connected for about 32 seconds. A picture of the battery after the test can be seen in Figure 4.3.

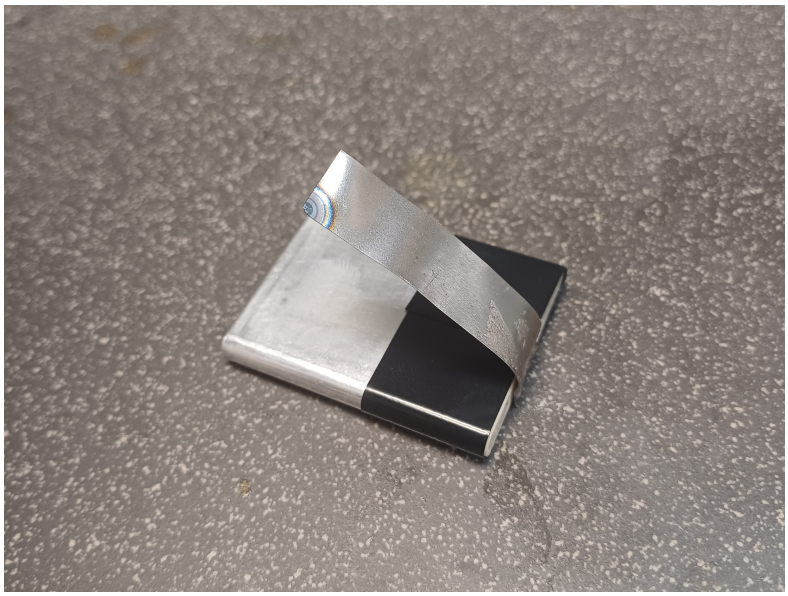

Figure 4.3. Li-ion cell after short test.

The LiPo's terminals were connected by holding a nickel strip against them. When connecting the terminals after the protection circuit module (PCM) circuitry, nothing happened except occasional sparks as the safety mechanism activated, and the printed circuit board (PCB) successfully prevented the short. To evaluate what would happen if the short happened before the protective PCB, the actual battery terminals were connected. The test lasted for about 10 seconds, and the battery heated up to 40 °C before the PCB started smoking, and the terminals were disconnected. The temperatures on the PCB rose up to the melting point of tin, as some components, including the cable of the positive terminal of the battery, unsoldered themselves. A picture of the battery and the PCB can be seen in Figure 4.4. The PCB was cut off due to safety reasons, as its wires had unsoldered themselves, which

could result in unexpected and dangerous behaviour.

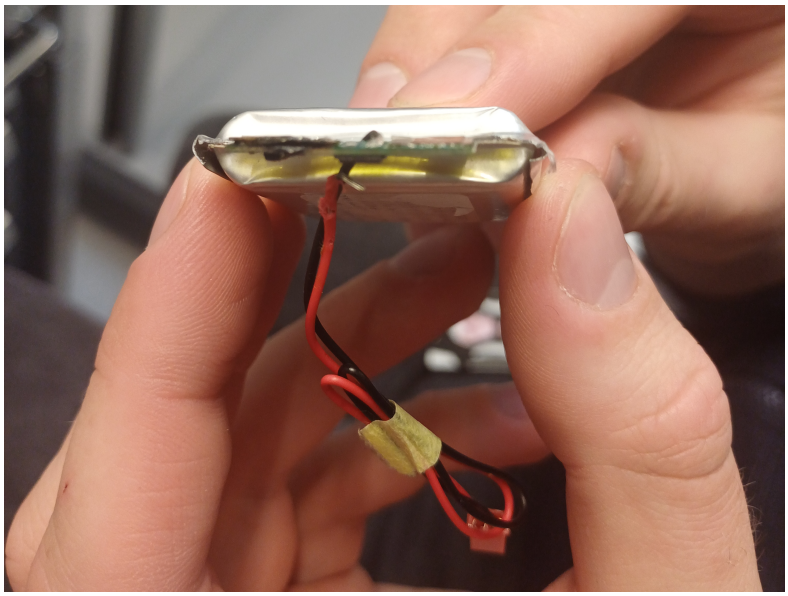

Figure 4.4. LiPo cell after short test.

Battery characteristics after the test were as follows in Table 4.6.

Table 4.6. Battery characteristics after the test

	Dimensions (mm)	Weight (g)	Voltage (V)
LiPo	38.13x37.77x10.10	27.2 (+1.5 PCB)	4.077
Li-ion	42.54x34.05x5.78	19.2	3.993

Overall, the batteries behaved as expected. The Li-ion battery heated up by a lot as it had no battery protection, but its dimensions stayed the same. Additionally, the Li-ion battery was successfully charged after the test. The LiPo battery's protective PCB worked well until it was bypassed and after that, the PCB broke.

4.3 Battery cell choice

The ACCU-LP103740/CL lithium-polymer battery includes a PCM that aligns well with the design requirements of the BatMan system. However, the battery has a soft case, meaning extra precautions should be taken when designing the battery module. Lithium polymer batteries are also known to expand because of their soft cases, which was proven in the vacuum tests. While this expansion did not result in critical failures during testing, it introduces an element of uncertainty. Furthermore, the

battery's single-sided terminal configuration complicates the mounting process, as it requires extra support at the base to ensure the battery will not come loose in its chassis. The battery's dimensions fit the predetermined criteria, but due to its width, the PCB the batteries would be mounted on would have little room for a connector.

In contrast, the UF553443ZU lithium-ion battery has a rigid metal casing and terminals located on both ends, simplifying the mounting process by allowing secure attachment on both sides. Although the body of the battery is charged positively, meaning the battery should be wrapped in tape to protect against unintended external shorts. The battery is also narrower than ACCU-LP103740/CL, leaving more room for a connector. The battery's thin case saves more space in the electronics stack, as stacking two batteries on top of each other to double their capacity is only 1 mm thicker than the LiPo battery, for 500 mA of extra capacity. The primary drawback of the UF553443ZU is its limited availability, as it is currently stocked only by a small electronics retailer in Estonia, raising concerns about its long-term availability.

Taking into account the points mentioned above, UF553443ZU will be chosen as the battery candidate, and ACCU-LP103740/CL will remain as the backup choice.

5 Prototype development and testing

5.1 Subsystem design

The first prototype of the subsystem was designed based on the ESTCube-2's battery management subsystem. The majority of the components were selected to be the same as on ESTCube-2, but alternative components were found if ESTCube-2's components did not fit the SUTS system parameters. The design consisted of four main blocks: the battery controller, voltage monitor, battery cut-off switch and the analog-to-digital converter (ADC). A simplified block diagram of the system configuration can be seen in Figure 5.1.

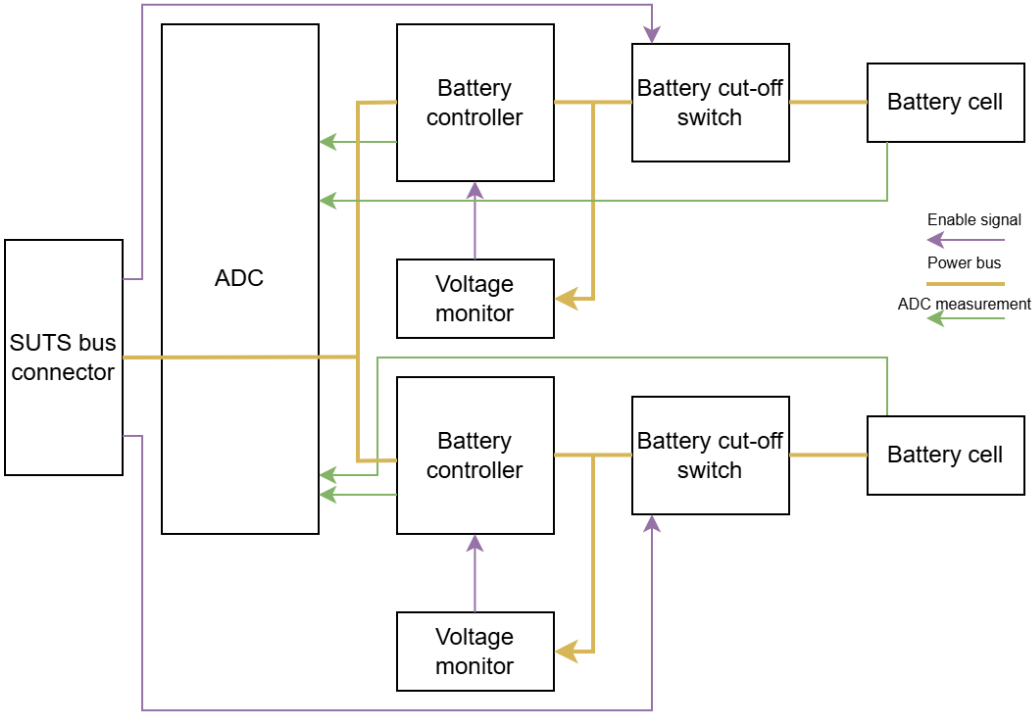

Figure 5.1. BatMan prototype system configuration.

5.1.1 Analog-to-digital converter

The purpose of the ADC is to monitor the charge and discharge currents, floating power bus voltage, battery voltages, and battery temperatures. The ADC used in the design is the 12-bit MAX1231 [17], which has an external voltage reference (ADR3425ARJZ-R7 [18]) connected to its REF+ pin, which has a constant value of 2.5 V. An external voltage reference was used instead of connecting the REF+

pin with the 3 V power bus to ensure that the value of the reference is constant. The 3 V power bus' constant value cannot be guaranteed, because it may change as the battery voltage changes. The reference value was chosen in such a way that it would always be lower than the ADC's supply voltage to comply with the chip's REF+ voltage range. The maximum value of the pin can be 50 mV over the supply voltage. Therefore, if the reference voltage is chosen to be too high and the supply voltage level falls within the range of the reference voltage, the REF+ pin could be damaged.

In addition, LMT84 [19] is used to measure the battery cell's temperature. The battery temperatures are measured from the longest side of the battery, where the temperature sensor is positioned against the battery. The ADC circuitry configuration can be seen in Figure 5.2.

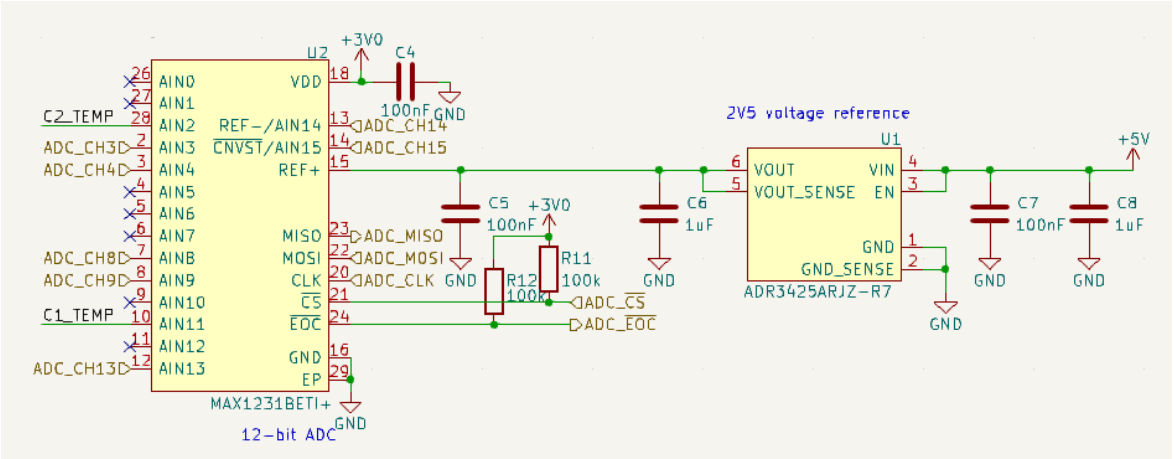

Figure 5.2. ADC circuitry configuration.

5.1.2 Battery controller

Battery charging and discharging are controlled by the LTC1647 [20] hot swap controller. The circuitry has external current sense monitors (LT6105 [21]) connected to the ADC. An image of the battery controller configuration can be seen in Figure 5.3.

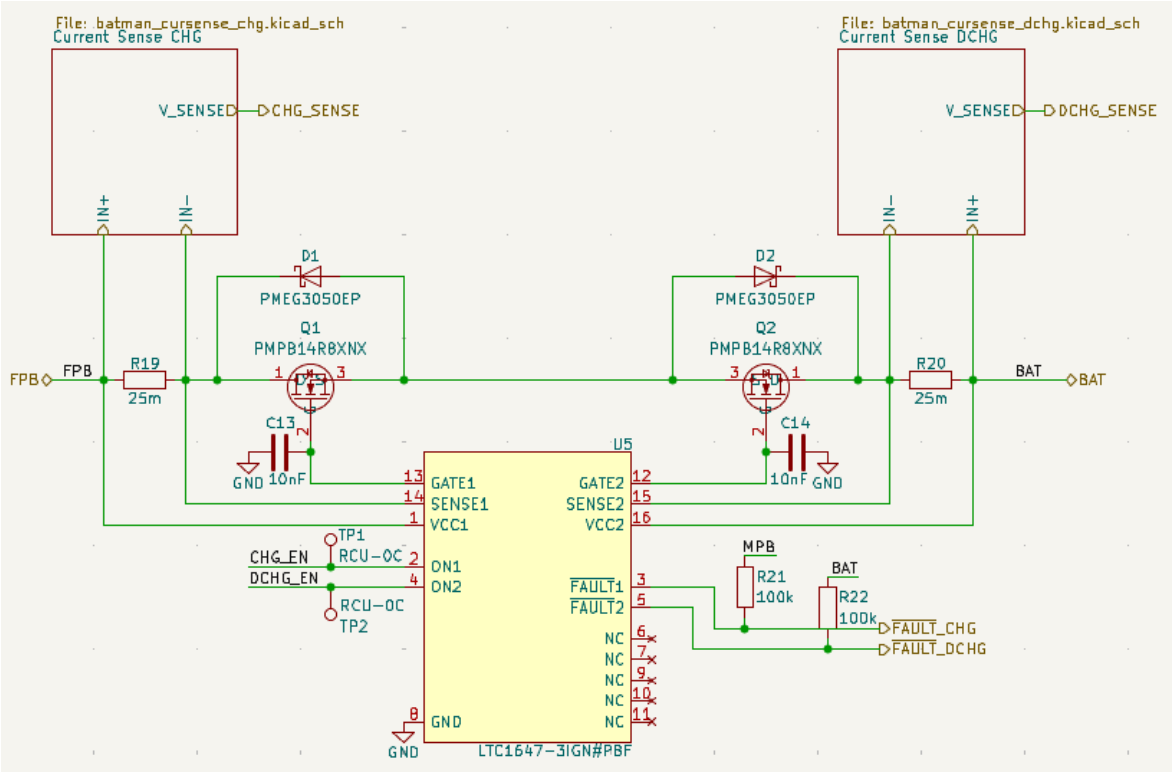

Figure 5.3. Battery controller circuitry configuration.

The resolution of the ADC is 2.5 V / 2^{12} = 610.4 uV. Therefore, with the LiPo configuration, the current resolution of charging is (610.4 uV / 51) / 33 mOhm = 0.36 mA (62 being the gain of the current sense), and the discharging resolution is (610.4 uV / 68) / 25 mOhm = 0.36 mA. The Li-ion configuration has a charging resolution of (610.4 mV / 51) / 25 mOhm = 0.48 mA and a discharging resolution of (610.4 mV / 47) / 25 mOhm = 0.52 mA. This represents the ideal scenario, assuming perfect performance of all electronic components. However, in real-world applications, the resolution is typically worse due to component tolerances.

5.1.3 Voltage monitor

As mentioned in Chapter 2.2, lithium batteries can only be used in the 3 V to 4.2 V voltage range. To ensure that the batteries remain in that range, TPS3700 [22] is used. TPS3700 measures the voltage on the battery rail and switches the battery controller output enable pins by comparing the battery rail with values preconfigured by the user. TPS3700 switches LTC1647 metal-oxide-semiconductor field-effect transistor (MOSFET) gates to enable or disable either the charging or discharging of the batteries. An image of the battery voltage monitor can be seen in Figure 5.4.

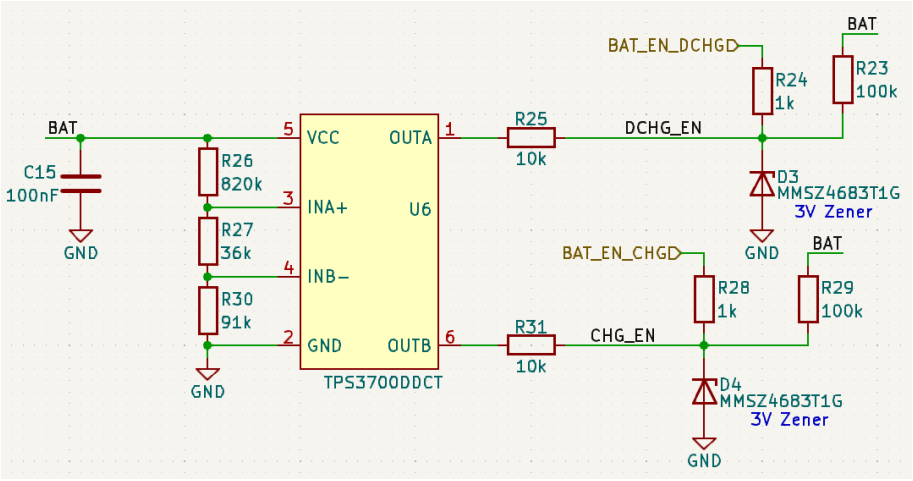

Figure 5.4. Battery controller voltage monitor circuitry configuration.

The maximum value of the battery rail should be 4.2 V, where charging is disabled (charge enable pin is pulled low). Once the battery rail voltage has gone down to 3.8 V (maximum value minus the threshold of 0.4 V), charging is enabled again. The minimum value of the battery rail should be 3 V, where discharging is disabled. Once the voltage level rises to 3.4 V (minimum value plus the threshold of 0.4 V), discharging is allowed again. When both charge and discharge enable pins are pulled high, current can flow freely on the battery rail. The charge and discharge level switching is illustrated in Figure 5.5.

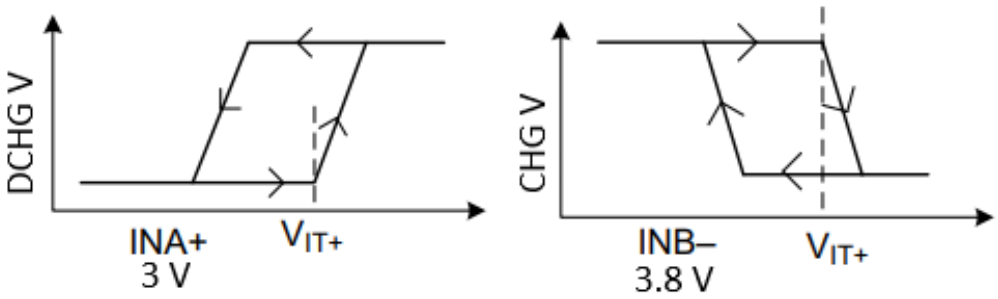

Figure 5.5. Voltage monitor switching logic.

These levels are set by three resistors between the VCC, INA+, INB- and GND pins of the chip. The datasheet [22] specifies the following equations to calculate these values:

$$VIT+ = 396(min)..400(typ)..404(max)mV \tag{5.1}$$

$$VIT- = 387(min)..394.5(typ)..400(max)mV \tag{5.2}$$

$$R30 = \frac{V_{IT+} \times R_{TOTAL}}{V_{OV}} \tag{5.3}$$

$$R27 = \frac{V_{IT+} \times R_{TOTAL}}{V_{UV}} - R30 \tag{5.4}$$

$$R26 = R_{TOTAL} - R30 - R27 \tag{5.5}$$

Where V_{OV} is 4.2 V, V_{UV} is 3 V, and R_{TOTAL} is 950 kOhm. Using these values, the following resistor values were acquired: R30 = 90.48 kOhm, R27 = 36.19 kOhm and R26 = 823.33 kOhm. These values were estimated to R30 = 91 kOhm, R27 = 36 kOhm and R26 = 820 kOhm to comply with the resistors available on site in Tartu Observatory.

5.1.4 Battery cut-off switch

LTC4231 [23] is used as an additional switch to cut off the battery from the main circuitry to minimise the parasitic currents that drain the battery when it is not in use. Additionally, it can monitor the voltage of the battery, cut it off from the rest of the system when the battery is undercharged, and reconnect it when it has reached safe charge levels. This function is not used, and the chip is only used as a cut-off switch. Although not all of the functionalities of this chip are used, it was chosen because it had already been tested onboard ESTCube-2.

The chip has an overvoltage protection feature, but it is not used in this case, as this feature would trigger the MOSFET connected to this chip to be turned off, leaving the battery in an overcharged state. As mentioned in Chapter 2.2, leaving a lithium battery in an overcharged state could damage the battery. To avoid triggering this condition, the overvoltage trip point is set to 10.97 V, which should never happen. The undervoltage trip point is set to be 2.886 V, and the undervoltage recovery point is 3.017 V. An image of the battery cut-off circuitry can be seen in Figure 5.6.

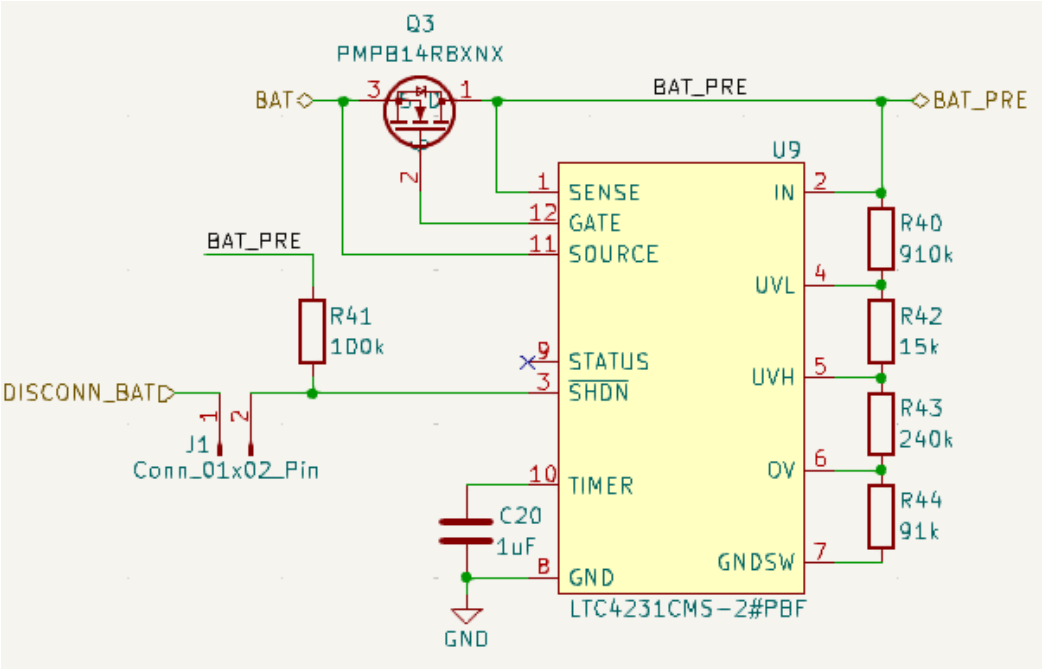

Figure 5.6. Battery cut-off circuitry configuration.

The voltage levels can be set by the following equations [23]:

$$V_{RANGE} = 0.776(min)..0.795(typ)..0.814(max)V \tag{5.6}$$

$$R_{TOTAL} = R40 + R42 + R43 + R44 \tag{5.7}$$

$$R44 = (\frac{V_{RANGE}}{V_{OVOFF}}) \times R_{TOTAL} \tag{5.8}$$

$$R43 = (\frac{V_{OVOFF}}{V_{UVON}} - 1) \times R44 \tag{5.9}$$

$$R42 = (\frac{V_{UVON}}{V_{UVOFF}} - 1) \times (\frac{V_{OVOFF}}{V_{UVON}}) \times R44 \tag{5.10}$$

$$R40 = (\frac{V_{OVOFF}}{V_{RANGE}} - 1) \times R44 - R43 - R42 \tag{5.11}$$

Where R_{TOTAL} is 1250 kOhm, V_{OVOFF} is 10.97 V, V_{UVOFF} is 2.886 V and V_{UVON} is 3.017 V. The calculated values are R44 = 90.59 kOhm, R43 = 238.8 kOhm, R42 = 14.95 kOhm and R40 = 905.67 kOhm. These values were estimated to R44 = 91 kOhm, R43 = 240 kOhm, R42 = 15 kOhm and R40 = 910 kOhm to comply with the resistors available on site in the Tartu Observatory.

5.2 PCB design

The schematic and PCB were made with KiCad [24] with the goal of the first prototype to just validate the design and make testing the circuit as simple as possible. The PCB was created so it could accommodate both battery candidates and the final design had two layers and was 150 x 94 mm in size. It was manufactured by JLC PCB, and the images of the PCB can be seen in Appendix B.

5.3 PCB assembly results

The PCB was assembled in the electronics laboratory of the Tartu Observatory, one functional block at a time, and the functionality of each block was tested before moving on to the next.

The ADC block, seen in Figure 5.2, worked as expected, as voltage readings could be captured from each ADC channel. The current sense chips worked as well, as the voltage readings that were obtained were proportional to the applied current through the current sense resistor. The voltage monitor also worked correctly, and it switched its charge/discharge outputs according to the battery voltage and set the window values.

5.3.1 Unexpected results

5.3.1.1 Battery controller

The battery controller sub-block, seen in Figure 5.3, did not work according to expectations; it signalled faults and behaved unexpectedly. The battery controller is supposed to switch its MOSFETs according to the logic values provided by the voltage monitor block. When the battery voltage is below 3 V, the MOSFET closer to the battery cell is supposed to be closed, blocking current from going out of the battery cell, and the other MOSFET is supposed to stay open. When the battery voltage is between 3 V and 4.2 V, both MOSFETs are supposed to stay open. Lastly, when the battery voltage is higher than 4.2 V, the MOSFET that is farther away from the battery cell is supposed to close and the nearer one is supposed to stay open to let the battery cell discharge.

When a load was applied to FPB, the MOSFET enabling battery discharge behaved according to its enable signal. However, the MOSFET controlling battery charge stayed closed, and chip indicated a fault on the corresponding fault pin. When adding the load on the other side of the circuitry i.e. to mimic the battery charge, the exact opposite happened - the charge MOSFET was enabled, but the discharge MOSFET was shut down. In the nominal case, when the voltage and current values are in

allowed ranges, the battery controller should keep both the charge and discharge MOSFETs open to enable power transfer from the battery to the FPB and vice versa. The MOSFETs should be closed only when an over- or an undervoltage situation occurs.

To figure out what was wrong with the logical block, a breakout board was milled out with Tartu Observatory's PCB mill, and it can be seen in Figure 5.7. The breakout board had just the battery controller and current sense chips to make sure no other components influenced the tests.

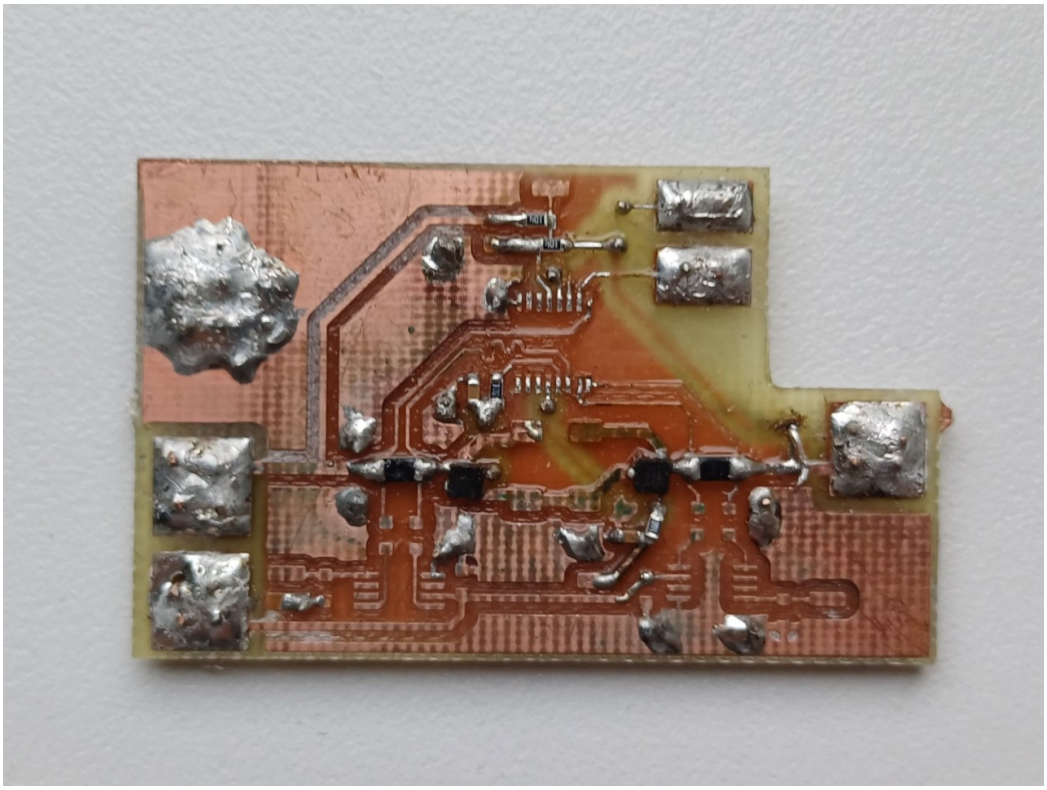

Figure 5.7. Battery controller breakout board.

It was discovered that the LTC1647 raises the gate voltage to above 10 V to force the MOSFETs open. Therefore, the MOSFET used in the initial design, PMPB14R8XNX [25], was not suitable for the design, as it had a gate-to-source voltage limit of 12 V. This did not leave a large enough margin and caused the MOSFETs to heat up in several tests. The MOSFETs were switched out for CSD17571Q2 [26] to prevent problems from operating too close to the gate-source voltage. Additionally, LTC1647's datasheet mentioned a 10-ohm resistor on the gate line, which was also added to the new design. Together with the capacitor between the gate and ground, the aforementioned resistor is a filter to lessen the ripple of the gate signal. Additionally, the bypass diodes in parallel with the MOSFETs were unsoldered to make sure all charge current flowing through the circuit would go through the two MOSFETs.

For the tests, the circuit was powered from the FPB side with 4 V, and different loads were placed

on the battery cell side to simulate different battery charging currents - 0 A, 100 mA and 500 mA. The fault pin levels, gate pin levels, and the voltage drop across the sense resistor were measured for during tests.

The expected behaviour would have been that noth MOSFETs be open, since a logical enable signal was added to both the charge and discharge enable pins of the battery controller. However, during all tests, the chip indicated a fault for both outputs. Fearing a broken chip, the battery controller was replaced with a brand new one and tests were repeated. Unfortunately, this chip produced test results identical to the behaviour that was noted on the initial PCB.

After testing, it was suggested that the chip may be faulting because it detects a reverse current on one of its current sense inputs - as the battery is charging, a reverse voltage is measured on the discharge path and when the battery is discharging, a negative voltage is measured on the charge path. After further consulting with the LTC1647's datasheet, an example circuit was copied from the datasheet and a breakout board was made. The aim of the breakout board was to prove that the chip works as intended when it doesn't measure reverse currents. Previously described load tests were repeated on the new PCB. The results of the test concluded that there are no faults in the circuitry when it is not under any load. However, when a load was applied to one outputs, the other charge path immediately indicated a fault. Meaning, these results did not prove the theory of the circuitry failing when a reverse current is applied. Therefore, the reason for the LTC1647 fault is still unknown and it was suggested to look into alternatives.

An alternative chip, LTC4368 [27], was suggested as a replacement for LTC1647. LTC4368 is a voltage controller that has built-in reverse protection. It also has a bidirectional current measuring function, which checks for overcurrent. Additionally, it has configurable overvoltage and undervoltage pins. This means that the voltage monitoring part of the circuit could possibly be removed in the future, making the design less complex and more compact. A design with LTC4368 will be designed and tested in the coming months and is outside the scope of this thesis.

5.3.1.2 Battery cut-off switch

The battery cut-off sub-block, seen in Figure 5.6, did not work correctly as it did not fully close the MOSFET when the circuit was told to disconnect. During testing, it was discovered that the MOSFET gate voltage was still around 0.2 V, which was near the MOSFET's gate threshold voltage, keeping it half open.

As ESTCube-2 had an identical configuration for its cut-off circuitry, the ESTCube-2 flatsat was

inspected. Two tests were conducted, first the LTC4231's shutdown pin was pulled high, meaning the MOSFET should have been open and current should have been flowing freely. During this test, the shutdown pin's voltage was 6.66 V, the gate voltage was 18 V, and the battery rail had 6.63 V. Thus, the results were as expected. For the second test, the shutdown pin was connected to ground, meaning the MOSFET should have been closed and the batteries disconnected. The measured shutdown pin voltage was 0 V, the gate voltage was 1.39 V, and the battery rail was 2.01 V. These, results were not as expected, as the gate should have been discharged to ground, and the battery voltage after the MOSFET should have been 0 V.

Another breakout board was made to test why the cut-off logical block did not work properly, and it can be seen in Figure 5.8.

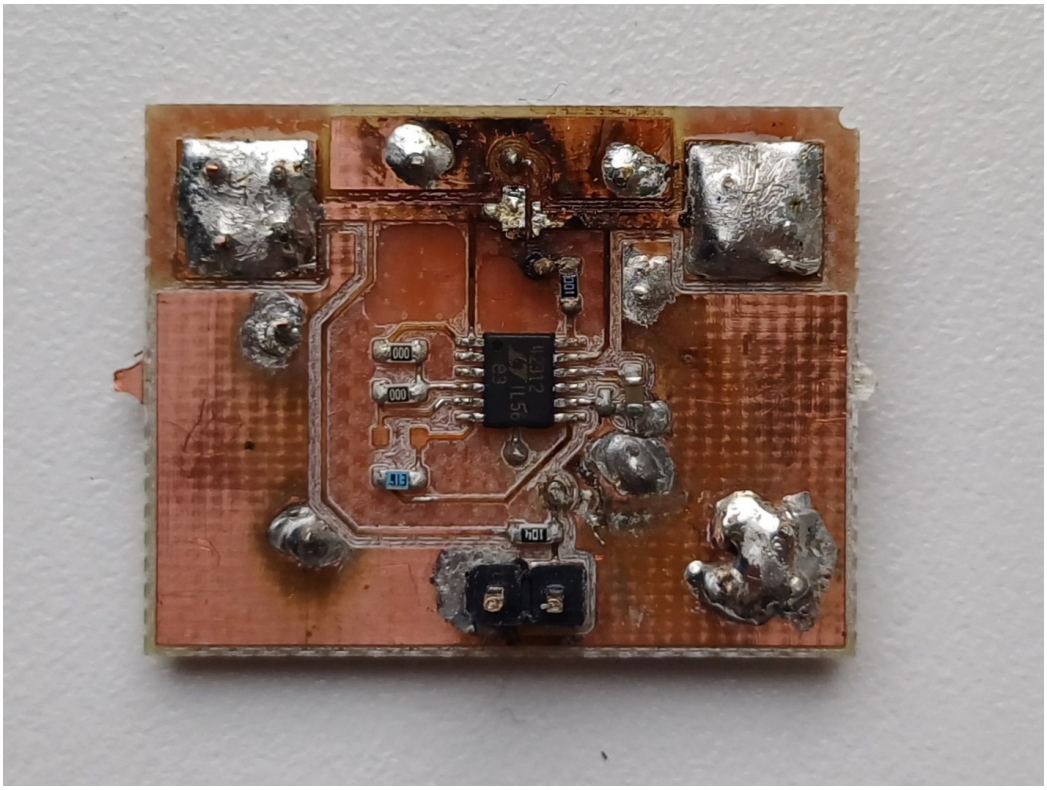

Figure 5.8. Battery cut-off switch breakout board.

The next step was to note down the current status of the SUTS circuitry. The battery voltage was simulated to be 3.7 V and a 0.9 A load was used. For the first test, the shutdown pin was high. The voltage measured on the pin was 3.66 V, gate voltage 5.06 V, battery rail after the MOSFET 3.61 V. The results were as expected. For the second test, the shutdown pin was shorted to ground. The voltage measured on the pin was 0 V, gate voltage 0.25 V and the battery rail 3.45 V. This showed that while the MOSFET was not as open as before, it still let current through and was not completely closed.

One of the possible reasons this was happening could have been because the MOSFET's threshold

voltage was too near to the voltage on the gate pin when the pin should have been in shutdown mode. Since the problem also appeared on ESTCube-2's flatsat, a fault in the chip was outruled. Although it is written in the chip's datasheet that during gate turnoff, a 1 mA pulldown current discharges gate to ground. In the end, an alternative MOSFET with a higher gate threshold voltage was found to make sure that the MOSFET is closed even if there is residual voltage on the gate pin.

The original MOSFET was replaced by CSD17571Q2. CSD17571Q2's gate threshold voltage was 1.6 V, and its limiting gate-to-source voltage was +/- 20 V. To test the work of the newly chosen MOSFETs, the voltage level monitoring functionality of LTC4231, the battery disconnect chip, was disabled by replacing certain resistors with 0 ohms and removing others. For all the tests, two values were recorded: battery line voltage after the disconnect MOSFET) and the MOSFET's gate pin voltage. After changing the original MOSFET to one that has a higher threshold voltage, the sub-block started working as expected and was therefore considered to be in working order.

6 Conclusions and future work

In this thesis, a design for the Battery Management Subsystem for the picosatellite SUTS was proposed. The three objectives of this thesis were to define the requirements of BatMan, find a suitable battery candidate for the system, and design and test the prototype BatMan. Eight requirements were defined for the battery management subsystem, ten battery candidates were found from various battery providers, and amongst them a final battery candidate, UF553443ZU, was chosen.

An electrical prototype was designed in KiCad to mimic the work of the final system and it was assembled at the Tartu Observatory laboratories. Multiple subblocks, including the ADC, voltage monitor, and battery cut-off switch, were successfully designed, assembled and tested. Although the battery controller encountered issues and wasn't fixed fully, the debugging process led to a potentially improved system design using an alternative component called LTC4368. For future work, the updated battery controller design will be implemented, assembled and verified. Once all battery management sub-blocks are tested, full environmental and integration testing can begin, ultimately leading to an engineering model of the flight system. In the long-term plan, this thesis marks an important milestone on the road towards SUTS' flight hardware development.

Bibliography

[1] *CubeSat Design Specification*. en. Feb. 2022. URL: https://static1.squarespace.com/static/5418c831e4b0fa4ecac1bacd/t/62193b7fc9e72e0053f00910/1645820809779/CDS+REV14_1+2022-02-09.pdf (visited on 31/10/2024).

[2] S. Radu, M. S. Uludag, S. Speretta, J. Bouwmeester, A. Dunn, T Walkinshaw, P.L. Kaled Da Cas, and C. Cappelletti. *PocketQube Standard*. en. 2018. URL: https://static1.squarespace.com/static/53d7dcdce4b07a1cdbbc08a4/t/5b34c395352f5303fcec6f1530184648111/PocketQube+Standard+issue+1+-+Published.pdf (visited on 31/10/2024).

[3] Martin N. Sweeting. „Modern Small Satellites-Changing the Economics of Space“. In: *Proceedings of the IEEE* 106.3 (Mar. 2018). Conference Name: Proceedings of the IEEE, pp. 343–361. ISSN: 1558-2256. DOI: 10.1109/JPROC.2018.2806218. URL: https://ieeexplore.ieee.org/document/8303876 (visited on 18/2/2025).

[4] *Power Systems*. en. URL: https://www.esa.int/Enabling_Support/Space_Engineering_Technology/Power_Systems (visited on 31/10/2024).

[5] Anil D. Pathak, Shalakha Saha, Vikram Kishore Bharti, Mayur M. Gaikwad, and Chandra Shekhar Sharma. „A review on battery technology for space application“. In: *Journal of Energy Storage* 61 (May 2023), p. 106792. ISSN: 2352-152X. DOI: 10.1016/j.est.2023.106792. URL: https://www.sciencedirect.com/science/article/pii/S2352152X23001895 (visited on 14/1/2025).

[6] A. J. Salkind, A. P. Karpinski, and J. R. Serenyi. „SECONDARY BATTERIES – ZINC SYSTEMS — Zinc–Silver“. In: *Encyclopedia of Electrochemical Power Sources*. Ed. by Jürgen Garche. Amsterdam: Elsevier, Jan. 2009, pp. 513–523. ISBN: 978-0-444-52745-5. DOI: 10.1016/B978-044452745-5.00172-6. URL: https://www.sciencedirect.com/science/article/pii/B9780444527455001726 (visited on 14/1/2025).

[7] Umberto Battista, Alberto Landini, Wojciech Gołebiowski, Rafał Michalczyk, Adam Czerwiński, Krzysztof Duda, and Agata Sochaczewska. „Design of net ejector for space debris capturing“. en. In: Apr. 2017. URL: https://www.researchgate.net/publication/

316789217_Design_of_net_ejector_for_space_debris_capturing (visited on 14/5/2025).

[8] Ratnakumar Bugga, Marshall Smart, Jay Whitacre, and William West. „Lithium Ion Batteries for Space Applications“. In: *2007 IEEE Aerospace Conference*. ISSN: 1095-323X. Mar. 2007, pp. 1–7. DOI: 10.1109/AERO.2007.352728. URL: https://ieeexplore.ieee.org/document/4161575 (visited on 6/5/2025).

[9] Barbara Mckissock, Patricia Loyselle, and Elisa Vogel. *Guidelines on Lithium-ion Battery Use in Space Applications*. Tech. rep. LF99-8857. NTRS Author Affiliations: NASA Glenn Research Center NTRS Document ID: 20090023862 NTRS Research Center: Langley Research Center (LaRC). May 2009. URL: https://ntrs.nasa.gov/citations/20090023862 (visited on 21/2/2025).

[10] *BU-402: What Is C-rate?* en. Feb. 2011. URL: https://batteryuniversity.com/article/bu-402-what-is-c-rate (visited on 12/3/2025).

[11] *BU-409: Charging Lithium-ion*. en. Sept. 2010. URL: https://batteryuniversity.com/article/bu-409-charging-lithium-ion (visited on 6/5/2025).

[12] Panasonic. *UF553443ZU Datasheet*. en. URL: http://www.alldatasheet.com/datasheet-pdf/view/597758/PANASONICBATTERY/UF553443ZU.html (visited on 4/5/2025).

[13] Zachary Cameron, Chetan S. Kulkarni, Ali Guarneros Luna, Kai Goebel, and Scott Poll. „A battery certification testbed for small satellite missions“. en. In: *2015 IEEE AUTOTESTCON*. National Harbor, MD, USA: IEEE, Nov. 2015, p. 8. ISBN: 978-1-4799-8190-8. DOI: 10.1109/AUTEST.2015.7356483. URL: http://ieeexplore.ieee.org/document/7356483/ (visited on 30/12/2024).

[14] *ECSS-E-HB-20-02A*. Oct. 2015. URL: https://ecss.nl/wp-content/uploads/2016/06/ECSS-E-HB-20-02A1October2015.pdf (visited on 4/2/2025).

[15] Guangxu Zhang, Xuezhe Wei, Jiangong Zhu, Siqi Chen, Guangshuai Han, and Haifeng Dai. „Revealing the failure mechanisms of lithium-ion batteries during dynamic overcharge“. en. In: *Journal of Power Sources* 543 (Sept. 2022), p. 231867. ISSN: 03787753. DOI: 10.1016/j.jpowsour.2022.231867. URL: https://linkinghub.elsevier.com/retrieve/pii/S0378775322008552 (visited on 3/1/2025).

[16] *Glass Lid Vacuum Chamber with Pump*. en. URL: https://bacoeng.com/products/glass-lid-vacuum-chamber-and-vacuum-chamber-with-pump (visited on 8/5/2025).

[17] Maxim Integrated. *12-Bit 300ksps ADCs with FIFO, Temp Sensor, Internal Reference*. 2012. URL: https://www.mouser.ee/datasheet/2/609/MAX1227_MAX1231-3468599.pdf (visited on 7/5/2025).

[18] Analog Devices. *Micropower, High Accuracy Voltage References*. en.

[19] Texas Instruments. *LMT84 1.5-V, SC70/TO-92/TO-92S, Analog Temperature Sensors*. en. Oct. 2019. URL: https://www.ti.com/lit/ds/symlink/lmt84.pdf?ts=1746621240082&ref_url=https%253A%252F%252Fwww.mouser.de%252F (visited on 7/5/2025).

[20] Linear Technology. *LTC1647-1/ LTC1647-2/LTC1647-3 Dual Hot Swap Controllers*. en. URL: https://www.mouser.ee/datasheet/2/609/1647fa-3124175.pdf (visited on 6/5/2025).

[21] Linear Technology. *LT6105 Precision, Extended Input Range Current Sense Amplifi er*. en. URL: https://www.analog.com/media/en/technical-documentation/data-sheets/6105fa.pdf (visited on 6/5/2025).

[22] Texas Instruments. *TPS3700 High voltage (18V) window voltage detector with internal reference for over and undervoltage monitoring*. en. Feb. 2019. URL: https://www.ti.com/lit/ds/symlink/tps3700.pdf?ts=1731999785456&ref_url=https%253A%252F%252Fwww.ti.com%252Fsitesearch%252Fen-us%252Fdocs%252Funiversalsearch.tsp%253FlangPref%253Den-US%2526nr%253D8%2526searchTerm%253DTPS3700DDCT (visited on 7/5/2025).

[23] Analog Devices. *LTC4231 Micropower Hot Swap Controller*. URL: https://www.mouser.ee/datasheet/2/609/LTC4231-1635151.pdf (visited on 7/5/2025).

[24] *KiCad EDA*. en-us. URL: https://www.kicad.org/ (visited on 6/5/2025).

[25] Nexperia. *PMPB14R8XN*. en. Oct. 2022.

[26] Texas Instruments. *CSD17571Q2 30V N-Channel NexFET Power MOSFETs*. en. Jan. 2015. URL: https://www.ti.com/lit/ds/symlink/csd17571q2.pdf?ts=1743661770490&ref_url=https%253A%252F%252Fwww.mouser.ee%252F (visited on 7/5/2025).

[27] Analog Devices. *LTC4368 100V UV/OV and Reverse Protection Controller with Bidirectional Circuit Breaker*. en. URL: https://www.analog.com/media/en/technical-documentation/data-sheets/ltc4368.pdf (visited on 8/5/2025).

[28] Large. *3.6V 2000mAh Explosion-proof Battery Panasonic Battery*. URL: https://www.large.net/product/8eu43cc.html (visited on 3/5/2025).

[29] Panasonic. *NCA673440*. June 2016. URL: https://en.actec.dk/media/documents/8F51BC221701.pdf (visited on 3/5/2025).

[30] *Keeppower IMR18350 High Drain*. URL: https://www.amazon.com/Keeppower-IMR18350-Battery-Rechargeable-Discharge/dp/B08HD3S16N (visited on 3/5/2025).

[31] Keeppower. *ICR18350-120PCM*. URL: https://www.tme.eu/Document/65828244a87e5a2ec4ACCU-IMR18350PCB.pdf (visited on 3/5/2025).

[32] Cellevia Batteries. *Specification Approval Sheet (LP103040)*. URL: https://www.tme.eu/Document/2167e0622fe5fe6f022823886e2ddddd/cel0118.pdf (visited on 3/5/2025).

[33] Cellevia Batteries. *Specification Approval Sheet (LP103740)*. en. URL: https://www.tme.eu/Document/ff228967c6b2684f2aeb29d2752e8d90/cel0107.pdf (visited on 3/5/2025).

[34] US Electronics. *Battery Specification*. URL: https://mm.digikey.com/Volume0/opasdata/d220001/medias/docus/5562/USE-903439-1400%20MAH.pdf (visited on 4/5/2025).

[35] XTAR. *XTAR AAA Lithium 1200mWh Battery with Low Voltage Indicator*. en. URL: https://www.tme.eu/Document/95ad3760cd85c938e9e1a2d6a8152483/XTAR-1.5V0.8AH-AAA.pdf (visited on 4/5/2025).

[36] *6ES7623-1AE01-5AA0*. ee. URL: https://ee.farnell.com/siemens/6es7623-1ae01-5aa0/rechargeable-batt-1-6ah-3-6v-lithium/dp/4008052 (visited on 4/5/2025).

[37] *XTAR LC4 Charger - XTAR*. en-US. URL: https://www.xtar.cc/product/xtar-lc4-charger-198.html (visited on 4/5/2025).

Acknowledgements

I would like to express my deepest gratitude to my thesis instructors, Mari Allik and Kristo Allaje, for supporting me throughout the process of writing this thesis, whether it was with your knowledge or with encouraging words. I could not have done it without you.

I would also like to thank Janis Dalbinš, Karl-Mattias Moor and Laur Edvard Lindmaa for helping me find solutions to my problems and giving general guidance and help. I would also like to thank the Student Satellite mentors, Viljo Allik and Kaspars Laizans, for giving me advice and feedback on my design, and the rest of the Student Satellite team for their support and help.

Lastly, I would like to thank my friends and family for their support in writing this thesis.

A Battery candidates

Battery	NCA103443		NCA673440		IMR18350		IMR18350		ACCU-LP103740/CL	
Capacity (mAh)	2010[28]	1	1265[29]	3	1200[30]	3	1200[31]	3	1580[32]	2
Dimensions (mm)	42.7x33.8x10.5[28]	1	40.35x33.8x6.75[29]	1	35(h),18.3(d)[30]	2	39(h),18.6(d)[31]	2	40x37x10[32]	1
Nominal voltage (V)	3.6[28]	1	3.6[29]	1	3.7[30]	1	3.7[31]	1	3.7[32]	1
Mass (g)	33.4[28]	3	20.3[29]	2	24.735[30]	2	26[31]	3	29.63[32]	3
Charge current (A)	$\leq$ 2.0[28]	1	0.854[29]	1	$\leq$ 1.1[30]	1	0.22[31]	2	$\leq$ 1.58[32]	1
Discharge current (A)	$\leq$ 2.95[28]	2	1.265[29]	1	10[30]	1	$\leq$ 8[31]	1	$\leq$ 1.58[32]	2
Charge temperature (°C)	10 - +45[28]	2	0 - +45[29]	1	?	3	?	3	0 - +45[32]	1
Discharge temperature (°C)	-20 - +60[28]	1	-20 - +60[29]	1	?	3	?	3	-20 - +60[32]	1
Notes	available on request from Actec; no datasheet	3	available on request from Actec; unreliable availability	1	no datasheet; 10.68€ in TME	2	has a PCM system included; 10.14€ in TME	0	LiPo; 10.99€ in TME	1
Sum of points	15		12		18		18		12	

Table A.1. First 5 battery candidates

Battery	ACCU-LP103040/CL		USE-903439-1400		10440 LI-ION AAA		6ES7623-1AE01-5AA0		UF553443ZU	
Capacity (mAh)	1200[33]	3	1350[34]	2	1200[35]	3	1600[36]	2	1040[12]	3
Dimensions (mm)	40.5x31.0x10.5[33]	1	41.0x34.5x9.5[34]	1	44.5(h),10.3(d)[35]	1	33(h),14.7(d)[36]	1	42.8x33.8x5.55[12]	1
Nominal voltage (V)	3.7[33]	1	3.7[34]	1	1.5[35]	3	3.6[36]	1	3.7[12]	1
Mass (g)	23.7[33]	1	24.5[34]	2	9[35]	1	14[36]	1	18.7[12]	1
Charge current (A)	1.2[33]	1	0.7[34]	1	0.5[37]	1	?	3	1[12]	1
Discharge current (A)	1.2[33]	2	0.28[34]	3	1.6[35]	2	?	3	1[12]	2
Charge temperature (°C)	0 - +45[33]	1	0 - +45[34]	1	0 - +45[35]	1	0 - +55[36]	1	0 - +40[12]	1
Discharge temperature (°C)	-10 - +60[33]	1	-10 - +55[34]	1	-20 - +60[35]	1	0 - +55[36]	2	-20 - +60[12]	1
Notes	Listed as hard to acquire; 8.91€ in TME	1	Shipped from the USA	3	4 pack in TME for 15.29€	0	177.04€ in Farnell; very vague datasheet	3	available in Tartu's Mobix for 17.60€	1
Sum of points	13		15		13		17		12	

Table A.2. Last 5 battery candidates

B PCB design

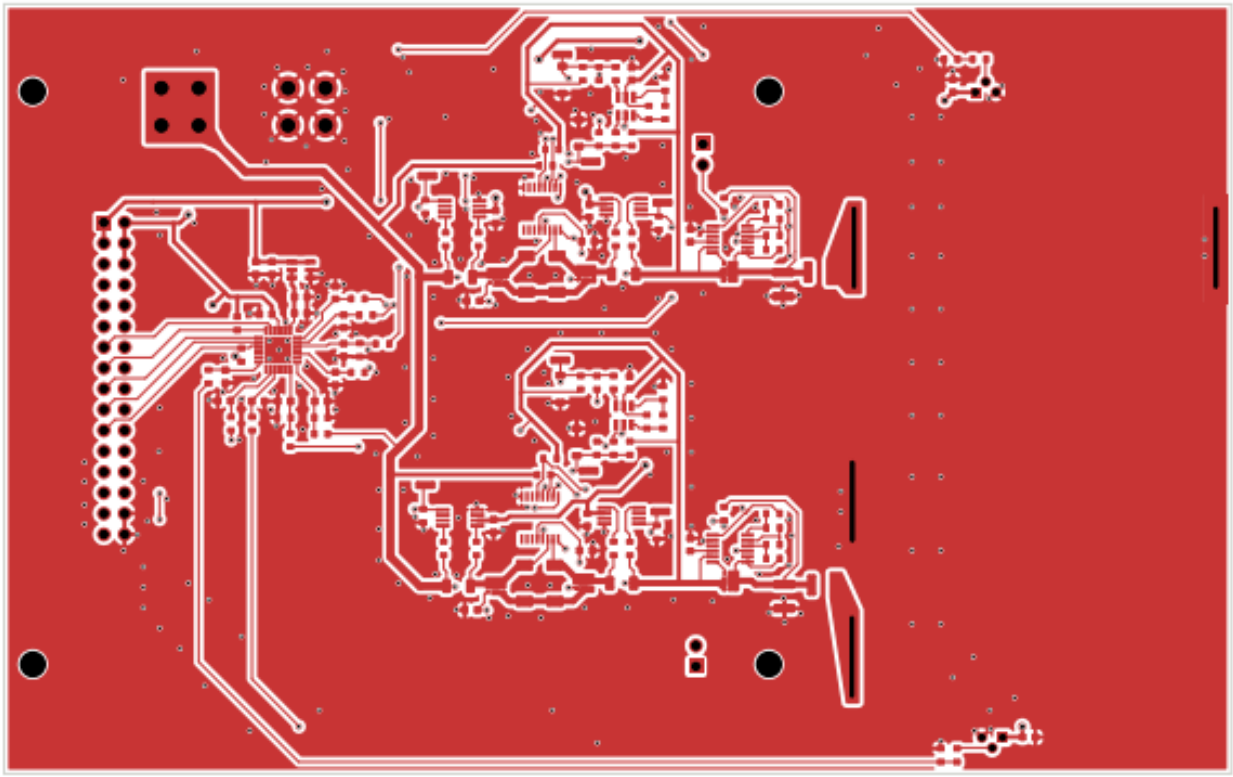

Figure B.1. Batman PCB front layer. This layer has all the components used on this PCB.

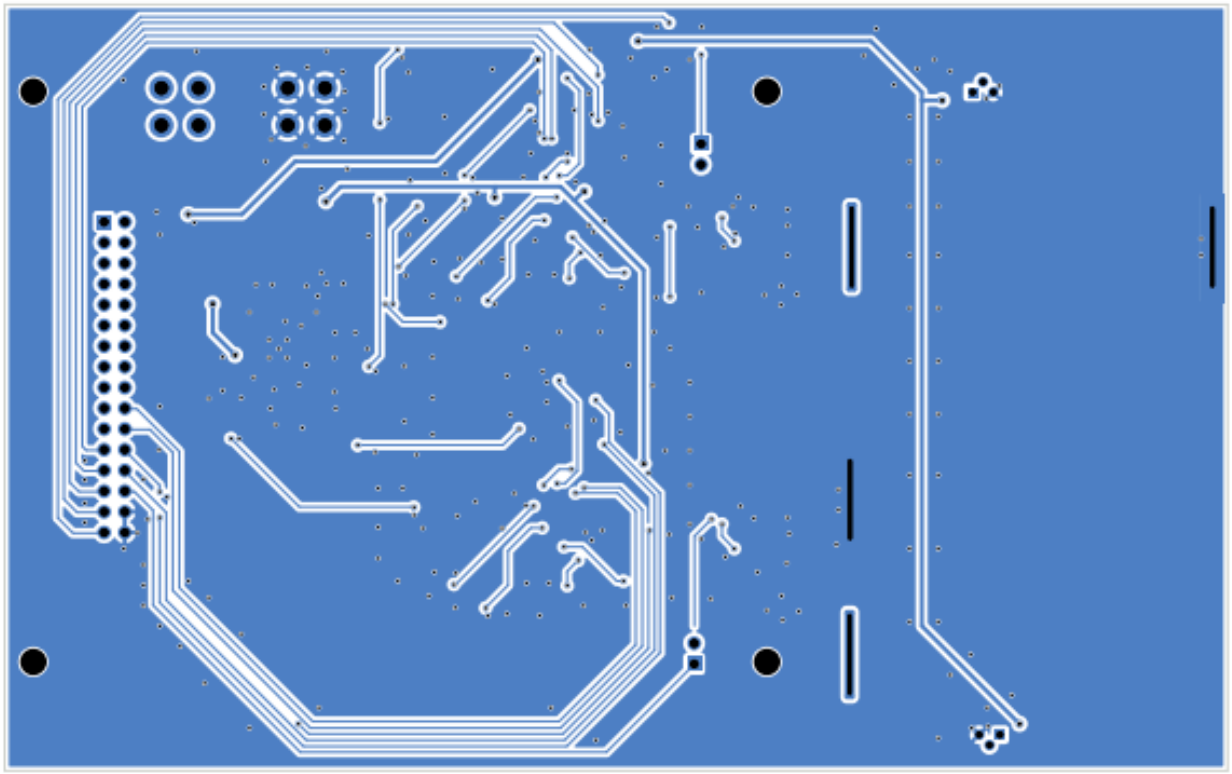

Figure B.2. Batman PCB back layer.

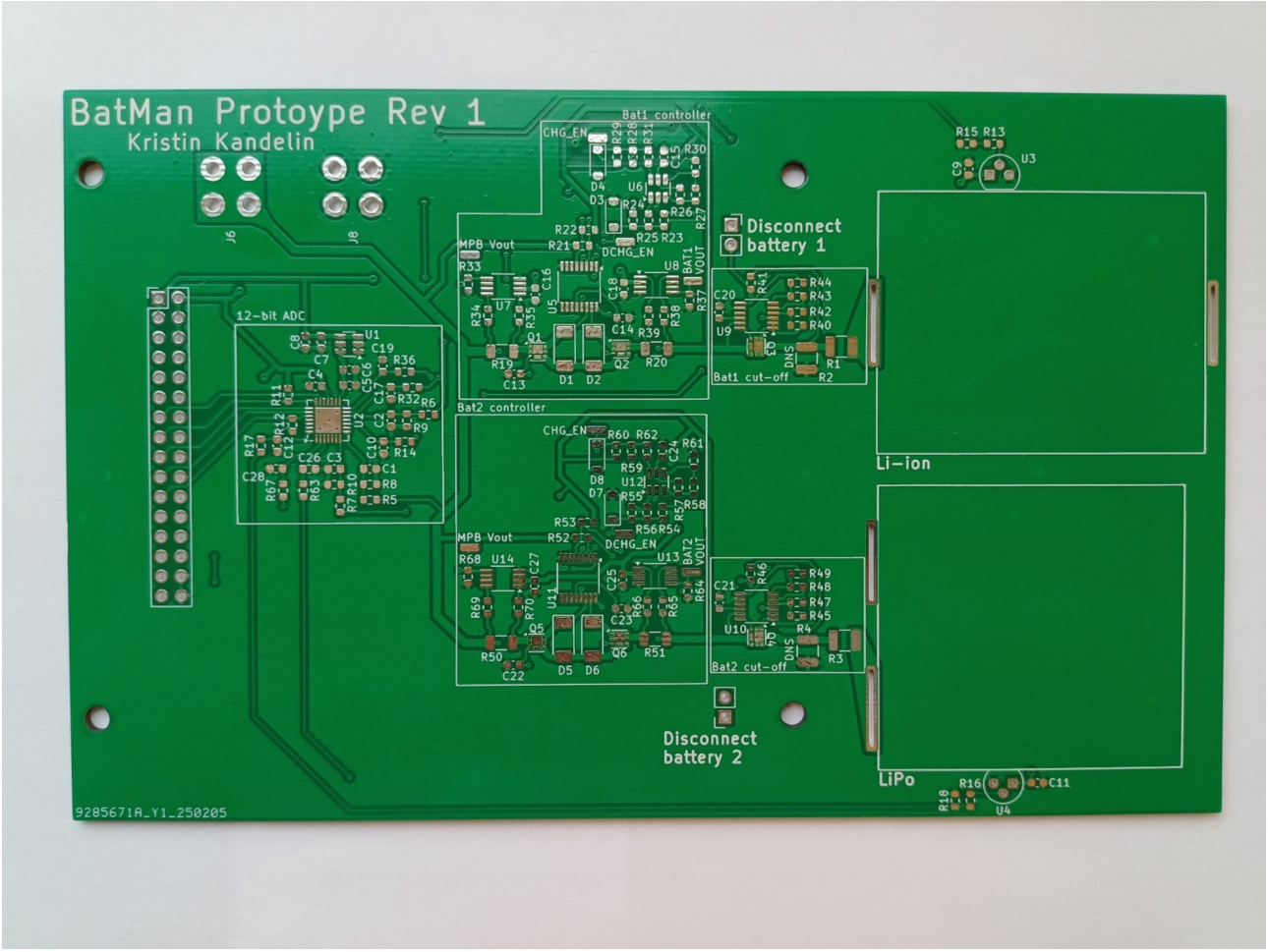

Figure B.3. Batman PCB from the front.

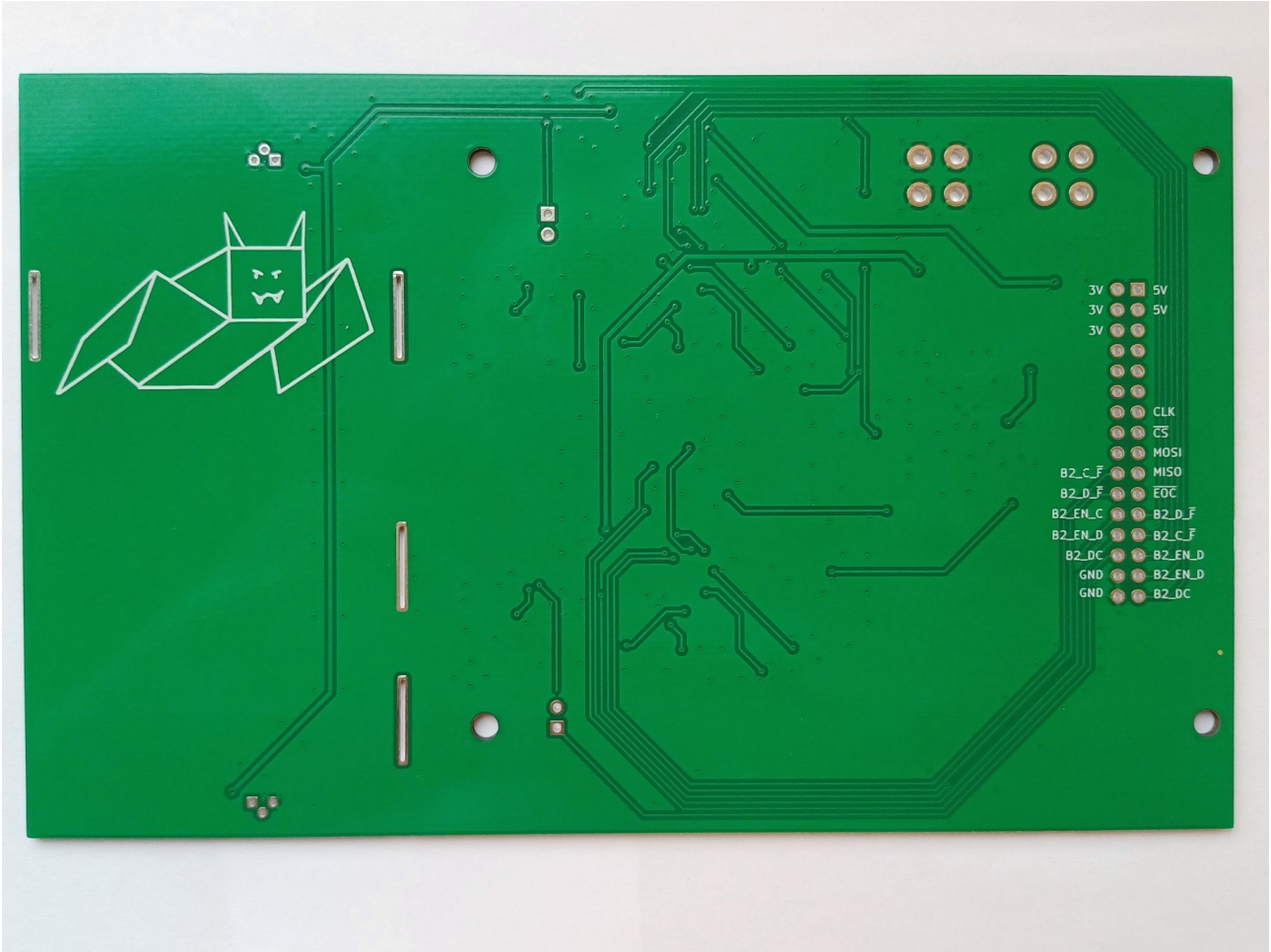

Figure B.4. Batman PCB from the back.

Licence

Non-exclusive licence to reproduce the thesis and make the thesis public

I, **Kristin Kandelin**,

1. grant the University of Tartu a free permit (non-exclusive licence) to
   reproduce, for the purpose of preservation, including for adding to the DSpace digital archives until the expiry of the term of copyright, my thesis
   "Development of the Battery Management Subsystem for the SUTS picosatellite"
   supervised by Mari Allik and Kristo Allaje

2. I grant the University of Tartu a permit to make the thesis specified in point 1 available to the public via the web environment of the University of Tartu, including via the DSpace digital archives, under the Creative Commons licence CC BY NC ND 4.0, which allows, by giving appropriate credit to the author, to reproduce, distribute the work and communicate it to the public, and prohibits the creation of derivative works and any commercial use of the work until the expiry of the term of copyright.

3. I am aware of the fact that the author retains the rights specified in points 1 and 2.

4. I confirm that granting the non-exclusive licence does not infringe other persons' intellectual property rights or rights arising from the personal data protection legislation.

Kristin Kandelin

20.05.2025